Revista Portuguesa de Diabetes. 2012; 7 (4): 192-197

Ecos do "47th EASD Annual Meeting" – Parte IV

Realizou-se, entre 12 e 16 de Setembro de 2011, no Centro de Congressos da Feira Internacional de Lisboa, no Parque das Nações, o "47th EASD Annual Meeting", maior congresso científico a nível mundial dedicado à diabetes, que reuniu, nesta edição, mais de 18.000 participantes de 120 países diferentes, na sua maioria profissionais de saúde ou investigadores biomédicos.

Dos 1.249 trabalhos científicos apresentados, 42 foram portugueses, número que corresponde a aproximadamente metade dos trabalhos científicos apresentados pelos norte-americanos, mas que foi superior ao dos trabalhos apresentado pela Suíça, o que mostra que a investigação nacional na área da diabetes se encontra em expansão.

Nesta parte IV da Revista Internacional dedicada ao "47th EASD Annual Meeting", concluímos a publicação dos "abstracts" dos trabalhos científicos apresentados por portugueses, por ordem de numeração no respectivo livro de "abstracts".

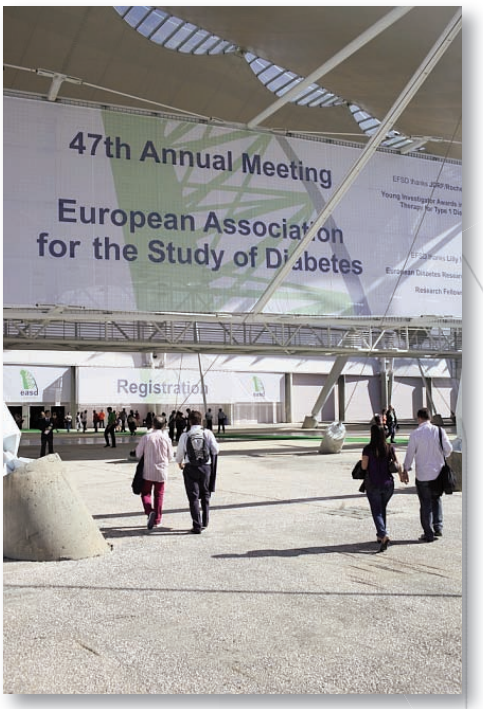

699

Noninvasive sampling of murine hepatic acetyl-CoA enrichment with p-amino benzoic acid

F. Carvalho (1), A. Gonçalves (1), J. Barra (1), M. Caldeira (1), J. Duarte (2,3), J. Jones (3,4)

(1) Chemistry, University of Coimbra, Coimbra, Portugal; (2) Advanced Imaging Research Center, UT Southwestern Medical Center, Dallas, TX, USA; (3) Center for Neurosciences, Coimbra, Portugal; (4) Associação Protectora dos Diabéticos de Portugal, Lisbon, Portugal

Background and Aims: Acetyl-CoA is a key hepatic metabolite but is difficult to analyze for enrichment from metabolic tracers. We developed a method that allows acetyl-CoA enrichment from 13C- and 2H-enriched precursors to be quantified. p-Amino benzoic acid (PABA) is acetylated via hepatic acetyl-CoA and N-acetyl PABA is cleared into urine where it is analyzed. To demonstrate this sampling method, acetyl-CoA enrichment from deuterated water (2H2O) was quantified by 2H NMR of N-acetyl-PABA in order to determine the true 2H-precursor enrichment for de novo lipogenesis. Second, the contribution of an [U-13C]glucose load to hepatic acetyl-CoA was determined by 13C NMR analysis.

Materials and Methods: In protocol 1, 4 mice were injected with 2H2O in saline (3g/kg body water) one hour into the light phase, and their drinking water was also enriched with 3% 2H2O. 24 hours later, they received an injection of PABA (15 mg/kg) dissolved in saline containing 3% 2H2O. Urine was collected for 6 hours following PABA injection. In protocol 2, 4 mice were fasted overnight, then injected with [U-13C]glucose (2 g/kg) and PABA (15mg/kg) in saline. Urine was collected over the following 6 hours. Urinary N-acetyl PABA was purified by solid phase extraction and the acetyl carbon and hydrogen enrichments from 2H2O and [U-13C]glucose were determined by NMR.

Results: Fig 1A and B shows representative 2H and 13C spectra of N-acetyl-PABA recovered from protocols 1 and 2, respectively. From protocol 1, enrichment of the acetyl CoA methyl hydrogens from 2H2O was estimated to be 2.2 ± 0.3 % compared to 2.4 ± 0.3 % for body water. This indicates that hepatic acetyl-CoA and body water enrichments were equivalent under these conditions. In Figure 1B, the 13C acetyl signals of the N-acetyl PABA is shown. For each carbon, the 13C-13C-coupled doublets (D), originating from the [U-13C]glucose precursor are well resolved from the background natural abundance 13C singlet (S) allowing the excess acetyl-CoA 13C-enrichment from [U-13C]glucose to be calculated. This was estimated to be 1.7 ± 0.1%.

Conclusion: Analysis of murine hepatic acetyl CoA enrichment from [U-13C]glucose and 2H2O by PABA administration and NMR analysis of N-acetyl-PABA was demonstrated. The analyses revealed that a surprisingly small fraction of hepatic acetyl-CoA (< 2%) was derived from an intraperitoneal glucose load given to 24-hour fasted mice. This suggests that the liver was not committed to glycolytic and lipogenic utilization of the administered glucose under these conditions. Following 2H2O administration, hepatic acetyl-CoA and body water hydrogens are enriched to the same levels hence body water enrichment can be used as a surrogate for the true acetyl-CoA precursor.

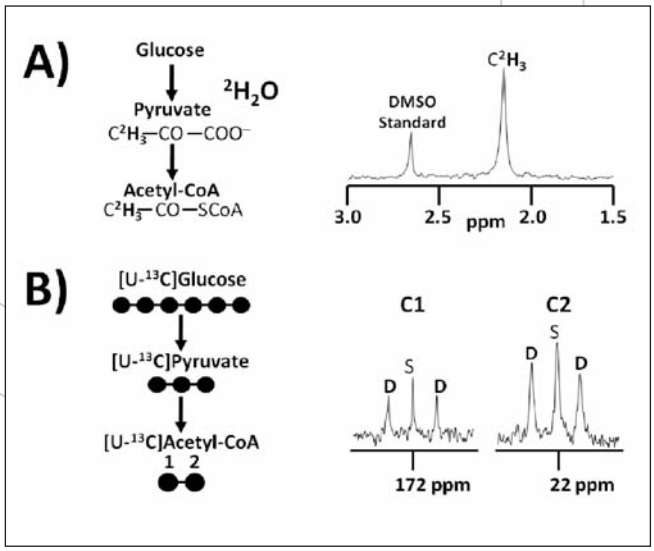

705

Regulation of hepatic lipid and cholesterol synthesis by PEPCK-C

J. A. G. Duarte (1,2), A. J. Potts (1), N. E. Sunny (1), S. Satapati (1), J. G. Jones (2), S. C. Burgess (1)
(1) Advanced Imaging Research Center, UT Southwestern Medical Center, Dallas, TX, USA; (2) Department of Life Sciences and Center for Neurosciences and Cell Biology, University of Coimbra, Coimbra, Portugal

Background and Aims: Cytosolic Phosphoenolpyruvate carboxykinase (PEPCK-C) catalyzes the conversion of oxaloacetate to phosphoenolpyruvate. Although this step is classically considered gluconeogenic, PEPCK-C is also expressed in non-glucose producing tissues like adipose tissue and is more generally a cataplerotic pathway required to match mitochondrial anaplerosis to biosynthesis and dynamic regulation of the TCA cycle. In addition to gluconeogenesis (GNG), PEPCK-C is important for glyceroneogenesis (GyNG), triglyceride (re)esterification and mitochondrial function. Despite being required for GNG, we previously demonstrated that the control coefficient of PEPCK-C over hepatic GNG is surprisingly low (0.18), but that complete loss of liver PEPCK-C causes impaired mitochondrial function. Liver-specific PEPCK knockout mice have a remarkable increase in hepatic triglyceride levels after an overnight fast, further underscoring the importance of this enzyme in the regulation of lipid metabolism. GyNG is a pathway that shares most enzymatic reactions with GNG and is critical for triglyceride synthesis. The objective of this study was to determine the consequence of PEPCK-C loss of function on the regulation of GyNG and its broader impact on lipid metabolism
Materials and Methods: Three types of mice with graded expression of PEPCK-C were used in this study: control (pck-1 lox/lox), 70% (pck-1 lox/neo) and 90% (pck-1 lox + neo/del) whole body knockdown and a liver specific PEPCK Knockout (pck-1 lox/lox+AlbCre). Mice were I.P. injected with 27ul/g 99.9% D2O to achieve a body water enrichment of 4% and then given 4% deuterated drinking water and chow ad libitum for 4-days to label hepatic and adipose triglycerides and cholesterol. Tissue triglycerides were extracts via Folch extraction and purified via solid phase extraction before being analyzed by 1H and 2H nuclear magnetic resonance (NMR). Synthesis of the glycerol and fatty acid moieties of triglycerides and cholesterol were determined from incorporation of deuterium compared to total deuterium body water enrichment.
Results: There was a direct correlation between synthesis fluxes and whole body PEPCK-C expression (see table). Remarkably, this correlation suggested a stronger control of fed state GyNG by PEPCK-C than we previously reported for fasted state GNG. Despite no obvious requirement for PEPCK-C in lipogenesis or cholesterogenesis, the synthesis of total FFA, unsaturated FFA and cholesterol strongly correlated with levels of PEPCK-C. This observation was most apparent in whole body PEPCK-C deficient mice and less evident in liver specific KO mice.
Conclusion: These data confirm an important role for PEPCK-C in glycerol and triglyceride metabolism and reveal an unexpected role for PEPCK-C in fatty acid and cholesterol synthesis.

Hepatic fluxes in animals with graded PEPCK. Data presented mean±SEM. *p<0.05 vs control

	lox/lox 100% PEPCK-C	lox/neo 30% PEPCK-C	lox + neo/del 10% PEPCK-C	lox/lox+AlbCre 0% PEPCK-C
Fatty acid synthesis (mg/day/g of liver)	13.93±1.09*	8.39±1.23*	6.39±0.53*	9.65±1.79*
glycerol synthesis (mg/day/g of liver)	7.35±0.97	6.49±1.13	4.14±0.71*	2.84±0.33*
Unsaturated fatty acid synthesis (mg/day/g of liver)	5.00±0.61	2.08±0.41*	1.73±0.16*	2.99±0.52*
Cholesterol synthesis (mg/day/g of liver)	115,22±17.78*	59.66±12.73*	43.78±7.53*	97.82±4.82*

717

Methylglyoxal causes structural and functional alterations in adipose tissue independently of obesity

P. Matafome (1,2), D. Santos Silva (1), J. Crisóstomo (1), T. Rodrigues (1), L. Rodrigues (1), C. M. Sena (1), P. Pereira (2), R. M. Seiça (1)
(1) Institute of Physiology, IBILI, Faculty of Medicine, University of Coimbra, Coimbra, Portugal; (2) Center of Ophthalmology, IBILI, Faculty of Medicine, University of Coimbra, Coimbra, Portugal

Background and Aims: Adipose tissue alterations including impaired adipocytokine expression, cell death, hypoxia and macrophage infiltration occur since early type 2 diabetes stages as it is the first organ to develop insulin resistance even on moderate BMI values. However, the contribution of hyperglycemia to these events during type 2 diabetes progression was never object of study. In this work we intended to evaluate the role of chronic hyperglycemia and specifically methylglyoxal (MG) on adipose tissue dysfunction.
Materials and Methods: We studied normal Wistar (W) rats and a non-obese model of type 2 diabetes, Goto-Kakizaki (GK) rats with 6 and 14 months old, in order to understand chronic effects of hyperglycemia and ageing. We also studied a group of W rats with MG administration (WMG) in order to study MG-specific mechanisms. Several functional and morphological aspects were assessed, namely adipocytokines, fibrosis, glycation, hypoxia and inflammation.
Results: Hyperglycemia (fasting and 2 hours after i.p. glucose administration) is intrinsic to our diabetic animal model (P<0,001) and resulted in structural adipose tissue alterations, namely fibrosis and accumulation of PAS positive components, exacerbated in aged animals. Although in a lesser extent, these alterations were also observed in aged W rats and in MG-treated group. Decreased adiponectin circulating levels (P<0,05) were observed in aged diabetic and MG-treated rats. Diabetic rats, aged W and WMG showed decreased Bcl-2/Bax ratio (P<0,05) and increased caspase 3 expression (P<0,05). Diabetic rats, aged W and WMG also had impaired VEGF/Ang-2 ratio (P<0,05). These alterations leaded to interstitial hypoxia quantified by pimonidazole staining (P<0,05) and decreased tissue irrigation quantified by Evans Blue infiltration (P<0,05). In aged diabetic rats hyperglycemia resulted in increased MCP-1 (P<0,05) expression and macrophage (F4/80: P<0,05) accumulation in adipose tissue, localized in glycated fibrotic regions. These events were also observed in W rats treated with MG, but not in the other groups.
Conclusion: Ageing causes several structural and functional modifications of adipose tissue also observable in early type 2 diabetes stages. However, chronic hyperglycemia- induced MG accumulation leads to macrophage recruitment for glycated fibrotic regions, common features of adipose tissue dysfunction models and obese or metabolic syndrome patients. Our results show that MG contributes to adipose tissue dysfunction during type 2 diabetes progression.

747

Adiponectinaemia, metabolic status, insulin secretion and insulin resistance in obese women: influence of weight loss

J. Silva-Nunes (1,2), L. Duarte (1), A. Oliveira (2), A. Melão (2), M. Brito (2), L. Veiga (2)
(1) Endocrinology Department, Curry Cabral Hospital, Lisbon, Portugal: (2) Escola Superior de Tecnologia da Saúde de Lisboa, Lisbon, Portugal

Background and Aims: Obesity is strongly associated with type 2 diabetes mellitus and prediabetes. Loss of the excessive fat mass is expected to improve glucose metabolism. Adiponectin is an adipokine which levels increase with fat mass loss. AIMS: 1) To compare variation (Δ) in adiponectin levels, in insulin secretion (IS) and insulin resistance (IR) indexes, and in anthropometric parameters and metabolic status changes in obese women during weight loss program, according to their initial status; 2) to assess the association between changes in adiponectin levels, IS and IR indexes with those in anthropometric parameters.
Materials and Methods: We studied 100 premenopausal obese women anthropometrically characterized. They were submitted to fasting blood

sample collection, followed by an oral glucose tolerance test (oGTT). We used one index of IR (homeostatic model -HOMA-IR), one of insulin sensitivity (Matsuda formula) and two IS indexes (homeostatic model -HOMA% beta and insulinogenic index -INS-i). Women entered in a weight loss program and were reassessed for all parameters after 6 and 12 months.
Results: Patients were characterized by mean age=34.1±8.2 yrs, BMI= 43.6±8 Kg/m^2, fat mass=54±15.1 Kg, waist circumference=117.7±15.2cm, waist:hip ratio (WHR)=0.88±0.08, adiponectin=6.86±3.21µg/ml, Matsuda= 3.69±2.54, HOMA-IR=4.42±3.65, HOMA%beta=262.1±174.9 and INS-i= 24.2±20.2. Normoglycemia (NG) was present in 71 patients, prediabetes in 19 and diabetes in 10. Eighty six patients were reassessed at month 6 and 67 accomplished the 12 months follow-up. No difference between metabolic status groups were observed for anthropometric or adiponectin variation between baseline and months 6 or 12. There was a significantly difference in metabolic status characterization between baseline and month 6 ($p<0.001$) and between baseline and month 12 ($p<0.001$). Between baseline and month 6 we observed that ΔHOMA-IR was positively correlated with Δwaist ($p<0.001$; $r=0.475$) and Δfat mass ($p<0.001$; $r=0.579$); ΔMatsuda were negatively correlated with Δwaist ($p<0.001$; $r=-0.473$), ΔWHR ($p=0.006$; $r=-0.333$) and Δfat mass ($p<0.001$; $r=-0.521$); ΔINSi were negatively correlated with Δwaist ($p<0.001$; $r=-0.427$), ΔWHR ($p=0.001$; $r=-0.385$) and Δfat mass ($p=0.002$; $r=-0.379$); we found a direct correlation between Δadiponectin and ΔMatsuda ($p=0.003$; $r=0.361$). Considering variations between baseline and month 12, we observed that ΔHOMA-IR was positively correlated with Δwaist ($p<0.001$; $r=0.792$), ΔWHR ($p<0.001$; $r=0.547$) and Δfat mass ($p<0.001$; $r=0.76$); ΔMatsuda were negatively correlated with Δwaist ($p=0.002$; $r=-0.479$), ΔWHR ($p=0.015$; $r=-0.393$) and Δfat mass ($p=0.005$; $r=-0.442$). Δadiponectin was negatively associated with Δwaist ($p<0.001$; $r=-0.448$) and Δfat mass ($p<0.001$; $r=-0.568$); however it was independently and inversely correlated with ΔHOMA-IR ($p=0.020$; $r=-0.367$).
Conclusion: In weight loss programs, obese women lose fat mass (with a subsequently increase in insulin sensitivity and insulin secretion) independently from their initial metabolic status. Adiponectin levels parallels insulin sensitivity indexes during the process of weight reduction, independently from the amount of fat mass loss. That might indicate a direct insulin-sensitizing effect of adiponectin.

914

Pharmacological characterisation of metformin-induced intestinal contraction

S. Silva(1,2), A. Henriques (1,3), L. Carvalho (4), R. Seiça (5),
C. Fontes-Ribeiro (2)
(1) Centre of Pharmaceutical Studies, Faculty of Pharmacy, Coimbra, Portugal; (2) Pharmacology and Experimental Therapeutics (IBILI), Faculty of Medicine, Coimbra, Portugal; (3) Department of Life Sciences, Faculty of Sciences and Technology, Coimbra, Portugal; (4) Institute of Pathology, Faculty of Medicine, Coimbra, Portugal; (5) Institute of Physiology, Faculty of Medicine, Coimbra, Portugal

Background and Aims: Diarrhea is one of the side effects commonly reported with metformin treatment. The cause of diarrhea is unknown. The aims of this study were: 1. To determine the contractile response of the rat isolated ileum to metformin and characterize pharmacologically the mediating receptor. 2. To verify the possible changes of the metformin-induced intestinal contraction in diabetic (DM) rats.
Materials and Methods: Ileum segments isolated from male Wistar rats were prepared for isometric contractile concentration-response (CR) curves (not cumulative) for metformin (1-36 µM) and 5-HT (0.1-60 µM). Frequency-response (FR) curves were obtained through electrical field stimulation (EFS). Two successive CR curves were performed, after 100 µM acetylcholine; 15 min before each dose of the second CR curve, 10 µM atropine, 1 µM mepyramine, 1 µM ketanserin, 1 µM SB 224,289, 1 µM ritanserin or 1 µM methiothepin were added; 300 µM hexamethonium, 1 µM tetrodoxin (TTX) and 250 µM NG-nitro-L-arginine were added. The same procedure was performed in Goto-Kakizaki (GK) rats, a non-obese animal model of DM2. In each assay, control segments were used with the appropriate solvent of each drug. Ileum segments were also used for histological section and immunohistochemical techniques to study the immunoreactivities of 5-HT1B and 5-HT2A receptors.
Results: Metformin, in therapeutic levels (6-36 µM), caused concentration-dependent contractions (Emax of 12.20±0.79 mN, n=48; pEC50 of 4.89±0.034, n=47); 36 µM metformin did not significantly change the rat ileum frequency-dependent contractile response to EFS suggesting a non-neuronal mechanism of action, which was confirmed by the unchanged metformin CR curve in the presence of hexamethonium and TTX. Moreover, the metformin CR curve was not significantly altered by atropine nor by NG-nitro-L-arginine, excluding the involvement of muscarinic receptors or NO, but mepyramine, an inverse agonist of the H1 histamine receptor, did significantly change the metformin-induced contraction. Concerning 5-HT receptors, ketanserin and SB 224,289 did not change the metformin-induced contraction, which means that 5-HT2A/2C and 5-HT1B receptors are not involved. However, methiothepin (a non-selective 5-HT receptors antagonist) and ritanserin (a non-selective 5-HT2 antagonist), almost abolished the metformin-induced intestinal contraction which proves the involvement of 5-HT receptors, namely 5-HT2B receptors. The effects of ketanserin and ritanserin on the metformin CR curve were also observed on the 5-HT CR curve. Furthermore the immunohistochemical studies did not reveal any immunoreactivity for the 5-HT2A receptor on the smooth muscle layers. In GK rats the ritanserin reduction of the metformin-induced intestinal contraction only became significant at the last metformin dose of the CR curve.
Conclusion: Since in the gut about 90% of serotonin is synthesized, stored and released mainly by enterochromaffin cells, we propose that metformin may trigger the release of monoamines from enterochromaffin cells and that somehow their function is impaired in the presence of DM2.

1068

Dietary restriction retards ageing and diabetes-related kidney injury

T. M. M. Louro, C. M. Sena, R. M. Seiça
Institute Physiology and IBILI, Faculty of Medicine, Coimbra, Portugal

Background and Aims: Aging is a biological process and is associated with various metabolic disorders, including type 2 diabetes. The incidence of type 2 diabetes has risen considerably in the past 2 decades and diabetic nephropathy is one of the most important microvascular complications observed in diabetes. It is known that dietary restriction has an important role in preventing age-related diseases. The main purpose of the study was to analyze the effect of dietary restriction on kidney function related with aging and type 2 diabetes.
Materials and Methods: Male control Wistar and diabetic Goto-Kakizaki rats, with 12 months of age, were divided in four groups: two groups of Wistar (W) and GK rats (GK) fed ad libitum and two groups of Wistar (WDR) and GK rats (GKDR) with dietary restriction up to 35% during 4 months. We analyzed the metabolic profile, pro-inflammatory [tumor necrosis factor-alpha (TNF-alpha), interleukin (IL)-6, interleukin (IL)-1beta] and fibrotic [transforming growth factor (TGF)-beta1] markers, AMP-activated protein kinase (AMPK) and sirtuin-1 (SIRT1) in all groups by ELISA and Western Blot techniques.
Results: Dietary restriction significantly reduced (22%, $p<0.001$) body weight in GK rats, and glycaemia 2h after glucose load (20% and 27%, $p<0.01$) and HbA1c (6%, $p<0.05$; 16%, $p<0.001$) in normal and diabetic rats. Dietary restriction significantly improved triglycerides (27%, $p<0.05$; 60%, $p<0.001$) and free fatty acids (FFAs) (71%, $p<0.001$; 45%, $p<0.05$) in normal and diabetic rats. Furthermore, dietary restriction reduced the levels of all pro-inflammatory and pro-fibrotic markers in Wistar (TNF-alpha 25%, $p<0.05$;IL-1beta 25%, $p<0.01$; IL-6 31%, $p<0.01$;TGF-beta1 5%, $p<0.05$) and GK rats (TNF-alpha 50%, $p<0.01$; IL-1beta 33%, $p<0.01$; IL-6 32.5, $p<0.05$ and TGF-beta1 5%, $p<0.05$). Noteworthy, the ratio phospho-AMPK/AMPK (38% and 33%) and the levels of SIRT1 (24% and 21%) in normal and diabetic rats were significantly increased by dietary restriction ($p<0.05$).
Conclusion: The present study suggests that dietary restriction improves the metabolic profile and kidney function by a mechanism that apparently involves SIRT1 and AMPK in aged normal W and diabetic type 2 GK rats.

1082

RBP4 has an early marker of renal dysfunction in diabetic patients

B. Almeida, Á. Coelho
Day Hospital for Diabetes and Metabolic Diseases, Coimbra Hospital Center, Coimbra, Portugal

Background and Aims: Fat tissue is viewed as an active endocrine organ with a high metabolic activity. Adipocytes produces and secretes several adipocytokines that play an important role in the metabolic control of diabetes and obesity. Retinol binding protein type 4 (RBP4) is produced by adipocytes and macrophages.
Materials and Methods: Between December of 2008 and October of 2010, 309 patients were recruited with mean age 51±13.5 years. They were divided in two groups: obese nondiabetic (n = 133) and diabetics (n = 177). The patients underwent anthropometric examination, with the determination of waist circumference, BMI and fat tissue using electric bioimpedance. The serum concentration of RBP4 was measured by nephelometry. Statistical analysis was made using the software SPSS vs. 17.
Results: Diabetics had higher urea, creatinine, triglycerides, alanine aminotransferase and gamma glutamyl transpeptidase values (7.2 ± 4.7 vs. 5.6 ± 1.6 mmol / L; 77.2 ± 30 vs 69.6 ± 18.6 mmol / L,; 1.8 ± 1.1 vs 1.5 ± 0.7 mmol / L; 44.6 ± 24.7 vs 32.3 ± 27.8 U/L; 51.9 ± 57.7 vs 33, 9 ± 45.6 U / L, p <0.05) and lower HDL-C (1.2 ± 0.4 vs 1.6 ± 0.4 mmol / L, p <0.05) in comparison with the group of obese. In both groups we found a positive correlation between BMI and body fat mass with CRP (r =0.294 vs r = 0.381, r = 0.384 vs r = 0.398, p <0.05). Diabetic patients had higher values of RBP4 in comparation with the group of obese patients (53,5±15,9 vs 46,9±17,8 mg/dl). Positive correlations were found with the urea and creatinine in both groups (r = 0.449 vs r = 0.498, r = 0.444 vs r = 0.62, p <0.01). Positive correlation with 24 hours proteinuria was observed in diabetic patients (r = 0.59, p <0.01) and in obese patients there was a positive correlation with triglycerides (r = 0.374, p <0.01). No correlations were found with the anthropometric parameters.
Conclusion: This study highlights the role of adipocytokine in the metabolic profile: RBP4 is an excellent early marker of renal dysfunction. In the future it can be used to assess microvascular complications in type 2 diabetic patients.

1116

Human versus an automated grading system (Retmarker) in diabetic retinopathy screening

V. Maduro (1), V. Genro (1), J. F. Raposo (1), J. Feijo (2), C. M. Oliveira (2)
(1) Ophthalmology, APDP, Lisbon, Portugal; (2) Critical Health, Coimbra, Portugal

Background and Aims: Evaluate the benefits of using automated grading system (Retmarker technology) in screening diabetic retinopathy and compare this system with the golden standard (human grading).
Materials and Methods: Anonymous retinal images (2 per eye) from 1092 patients screened in 2009 and 2010 were obtained using a non-mydriatic 45-degree fixed Cannon-45NM camera on a Diabetic Retinopathy screening program run by APDP. Images were taken and graded by 3 experienced ophthalmologist. Additionally, images were evaluated by an automated grading system - Retmarker -and classified as "Disease", "No disease". Retmarker technology performs a 2-step analysis based on the detection of Microaneurysms and Lesion Activity (progression) within the macular region. Results of the automated analysis were compared with those obtained by manual grading.
Results: The Retmarker software classified, from de 1092 patients, 539 (49,4%) as having " Disease" and 553 (50,6%) as having "No disease", thus requiring manual grading. Retmarker achieves a sensitivity of 81.4% and a specificity of 52% with a negative predictive value of 98.6% and a positive predictive value of 6.5% when compared human grading based on patient referral criteria. A total of 8 cases marked by the human grading as having signs of Diabetic Retinopathy were not detected by the automated system, out of the 1092 patients (0.73%).
Conclusion: Automated grading of diabetic Retinopathy may safely reduce the burden of grading patients with and without disease in Diabetic Retinopathy screening programs. The novel two-step automated analysis system using Retmarker has the capability to reduce the human workload of grading by approximately 50,6%, while achieving a high sensitivity of 81,4%. Applying an automated program, such as the described one, an important reduction in the number of cases the expert needs to address is achieved, and thus there is an associated cost saving. Most importantly, an automated system, although not providing full detection, provides consistency by removing subjectivity.

1117

Validation of a predictive model for diabetic retinopathy progression in type-2 diabetic patients with mild NPDR

S. Nunes (1), R. Bernardes (2,3), T. Santos (2), I. Pires (4), C. Lobo (3,4), J. Cunha-Vaz (5)
(1) Coimbra Coordinating Centre for Clinical Research, Association for Innovation and Biomedical Research on Light and Image (AIBILI), Coimbra, Portugal; (2) Centre of New Technologies for Medicine, Association for Innovation and Biomedical Research on Light and Image (AIBILI), Coimbra, Portugal; (3) Institute of Biomedical Research on Light and Image (IBILI), Faculty of Medicine, University of Coimbra, Coimbra, Portugal; (4) Centre for Clinical Trials, Association for Innovation and Biomedical Research on Light and Image (AIBILI), Coimbra, Portugal; (5) Association for Innovation and Biomedical Research on Light and Image (AIBILI), Coimbra, Portugal

Background and Aims: To validate a predictive model for diabetic retinopathy progression in type-2 diabetic patients with mild NPDR using non-invasive examinations.
Materials and Methods: Four-hundred and twelve (412) type-2 diabetic patients with mild NPDR were included in this 2-years observational and prospective study. Three hundred and seventy-four (374) patients completed the first 6-month of follow-up and underwent: color fundus photography, retinal thickness (RT) measurements and blood tests. Microaneurysm formation rate (MAFR) was computed from color fundus photographs using a new automatic method for MA earmarking (RetmarkerDR, Critical Health SA.). Increased RT maps (Stratus OCT, Zeiss Meditec Inc.) were computed using proprietary software.
Results: Three hundred and seventy-one (371) patients were included in the analysis (1 patient was lost of follow-up and 3 patients were treated with laser photocoagulation before the 6-month visit). Patients were distributed according to RT values and MAFR into 3 distinct DR phenotypes: Phenotype 1 (low MAFR and normal RT); Phenotype 2 (low MAFR and increased RT) and; Phenotype 3 (high MAFR). One hundred and fifty (150, 40.4%) patients were assign to Phenotype 1, 116 (31.3%) to Phenotype 2 and; 105 (28.3%) to Phenotype 3. Clinically significant macular edema occurred during the follow-up period only in eyes from phenotype 2 (9 eyes, 7.8%) and phenotype 3 (7 eyes, 6.7%).
Conclusion: Our preliminary data confirms the existence of 3 different phenotypes of DR progression, as previously proposed, and simultaneously shows a similar distribution although using a different population.

1161

Diabetic foot ulcer risk stratification systems: Which one to choose? A validation study

M. Monteiro-Soares, R. Guimarães, A. Távora, E. Lemos, I. Duarte, J. Sobral, J. Campos-Lemos, D. Brandão, M. Madureira, M. Ribeiro, M. J. Oliveira;
Endocrinology, Diabetes and Metabolism, CHVNG / Espinho EPE, Vila Nova de Gaia, Portugal

Background and Aims: Diabetic foot ulcer (DFU) risk stratification systems are a crucial tool for diabetic foot care, screening, resource allocation and complications' prevention. There are various systems with different characteristics and a recent systematic review has shown that little has been done for their validation and comparison. In fact, some of them were never externally validated nor their prognostic accuracy reported. Therefore, choosing which one to apply in our setting may not be straightforward. Thus, this study aims to validate and compare all the available systems [the

University of Texas (UT), American Diabetes Association (ADA), International Working Group on the Diabetic Foot (IWGDF), Scottish Intercollegiate Grouping Network (SIGN) and Boyko and colleagues) for DFU occurrence prediction at 1 year (the lowest risk group recommended reevaluation).
Materials and Methods: A retrospective cohort study was conducted on all patients with diabetes but without active DFU attending the CHVNG/Espinho EPE Diabetic Foot Clinic, from March 2006 to March 2011 (n = 270). Characterization variables (age, gender, diabetes' duration, type and treatment) and all those included in the stratification systems were assessed and registered at baseline [HbA1C, neuropathy and peripheral vascular disease, foot deformity, callus, visual and physical impairment, onychomycosis, tinea pedis, previous DFU and lower extremity amputation (LEA)]. Later, variables were collected from the patients' clinical files from mid to end of March 2011. All systems were applied at the data collection moment. Participants were followed for 1 year or until DFU occurred, i. e., a full-thickness skin defect distal to the malleoli requiring more than 14 days to heal. Variables' distribution was compared between the groups of patients with and without ulcers over the follow-up course, using the appropriate statistical tests (according to the variables' type and normality of distribution). Significance was defined as $p < 0.05$.
Results: Type 2 diabetes was present in 99.6% of patients, 44,2% were men and (at baseline) the median age was 66 years and diabetes duration 16 years. Median follow-up was 12 months (range 1-12) during which 29 participants (10.7%) developed a DFU. Variables associated with DFU occurrence at 1 year were age, HbA1C, Semmes-Weinstein monofilament and/or tuning fork sensitivity alteration, number of pulses present, previous DFU or LEA. For all the systems there were more ulcerations as the risk group increased ($\chi 2$ for association and trend $p < 0.001$). The UT system presented an area under the receiver operating curve (AUC) of 0.70 [95% confidence interval (CI) 0.58-0.81], the ADA system of 0.82 (95% CI 0.77-0.88), the IWGDF system of 0.84 (95% CI 0.77-0.91), the SIGN system of 0.75 (95% CI 0.68-0.82) and the Boyko and colleagues system of 0.82 (95% CI 0.74-0.90).
Conclusion: There are several risk stratification systems that can be used in clinical practice to detect those at higher risk of DFU occurrence and they seem to be equally accurate. Although the selection of which system to apply is still unclear, this study shows that all of these systems present a high accuracy and therefore are a valuable tool. Nevertheless, further validation studies should be performed in larger samples and in different settings. There is also a great need to assess the reliability of the systems and their components.

1172

Neurotensin decreases TNF alpha-induced cell death in keratinocytes and macrophages: possible important role in diabetic wound healing

E. Carvalho, V. Maio, E. Leal
Center for Neurosciences and Cell Biology, University of Coimbra, Coimbra, Portugal

Background and Aims: Neuropeptides are known to be important in wound healing, particularly in diabetic wound healing. Although the role of neurotensin in wound healing is not well known. Moreover, a chronic inflammatory state in diabetes is responsible for the impairment of wound healing and tumor necrosis factor-alpha (TNF-alpha) appears to have an important role. In this study we aim to investigate the effects of neurotensin in TNF-alpha-induced changes in skin cells, keratinocytes and macrophages.
Materials and Methods: Keratinocyte (HaCat) and macrophage (Raw 264.7) cell lines were incubated with 10ng/ml of TNF-alpha and/or 100 nM of neurotensin for 6 and 24h. We evaluated cell viability with the MTT assay and cell death with nuclear staining (DAPI). Caspase-3, p38 MAPK, NFκB activation and the detection of oxidized carbonyl groups were evaluated by western blot. Nitrosative stress was detected with nitrotyrosine staining.
Results: We found that 24h of incubation with TNF-alpha decreased HaCat and Raw cell viability (78.7 ± 4.0 % and 82.8 ± 4.6% of control, $p<0.05$, respectively) and also caused cell death (6.2 ± 0.8% and 4.3 ± 0.3% of total cells, $p<0.05$, HaCat and Raw cells respectively). These effects were reverted by neurotensin. The active form of caspase-3 was found to be significantly increased with TNF-alpha in both cell types (HaCat, $p<0.05$, 369 ± 84.4% of control; raw, $p<0.01$, 329.2 ± 50.4% of control) and neurotensin decreased this activation suggesting that caspase-3 is involved in cell death. Neurotensin decreased TNF-alpha-induced activation of the p38 MAPK and NFκB pathways. In addition, neurotensin decreased TNF- alpha -induced oxidative and nitrosative stress in skin cells.
Conclusion: Neurotensin inhibits the TNF-alpha-induced decrease in skin cell viability and cell death. The protective effects of neurotensin appear to be mediated by a decrease in oxidative and nitrosative stress, and by the inhibition of caspase-3, p38 MAPK and the NF-kB pathways. These results suggest that neurotensin can have a protective role in chronic inflammatory conditions, particularly in chronic diabetic wounds.

1227

Vasoprotective effects of caloric restriction in aging and type 2 diabetes

R. M. Seiça (1), T. M. Louro (1), A. M. Pereira (1), D. Carvalho (1),
R. Fernandes (2), C. M. Sena (1)
(1) Institute of Physiology, IBILI, Faculty of Medicine, University of Coimbra, Coimbra, Portugal; (2) Institute of Pharmacology and Experimental Therapeutics, IBILI, Faculty of Medicine, University of Coimbra, Coimbra, Portugal

Background and Aims: Caloric restriction (CR) without malnutrition extends life span in a range of organisms including insects and mammals and lowers free radical production by the mitochondria. The direct effects of CR on vascular function and phenotype in aging are not well characterized. It is generally accepted that tonic release of nitric oxide (NO) from the endothelium exerts vasculoprotective and cardioprotective effects. The current study was undertaken to examine the effects of caloric restriction on endothelial function, metabolic, glycation and oxidative stress markers, in old age Wistar and diabetic Goto-kakizaki (GK) rats.
Materials and Methods: Wistar (W) and GK rats with twelve months old were progressively subject to CR up to 35% during 4 months and compared with ad libitum fed rats. The effects of CR were investigated on NO-dependent and independent vasorelaxation in isolated rat aortic arteries from the different groups. Metabolic profile, NO bioavailability, the accumulation of advanced glycation end-products (AGEs) and carboxymethylisine (CML), the expression of the receptor for AGEs (RAGE) in the aorta and vascular oxidative stress were also evaluated.
Results: We have previously shown that aging was associated with increased endothelial dysfunction in both W and diabetic GK rats. In this work we show that GK rats exhibited a three-fold increment in vascular oxidative stress and in CML accumulation when compared with age-matched W rats. Diabetes-induced excess accumulation of reactive oxygen species in aorta resulted in vascular nitric oxide (NO)/cGMP dysfunction (decrement of 40 %, $p<0.001$). Caloric restriction was able to retard the progression of endothelial dysfunction and significantly reduce aortic oxidative stress ($p<0.001$) in W and diabetic GK rats. Furthermore, CML accumulation in aortic wall was sharply reduced and accompanied by a decrement in the expression of aortic RAGE in caloric-restricted fed animals. Noteworthy, the NO-cGMP pathway in the aorta of GK rats was partially reverted explaining the positive outcomes observed in the endothelial function of diabetic GK rats.
Conclusion: This study provides, to our knowledge, the first evidence that caloric restriction increases bioavailability of NO improving endothelial function by a mechanism that likely includes upregulation of eNOS and a decrement in glycation and oxidative biomarkers in aged type 2 diabetic rats.

1259

The role of methylglyoxal in diabetic and normal cardiac ischaemia

J. Crisóstomo (1), P. Matafome (1,2), D. Santos-Silva (1), L. Rodrigues (1),
C. M. Sena (1), P. Pereira (2), R. M. Seiça (1)
(1) Institute of Physiology, IBILI, Faculty of Medicine, Coimbra, Portugal; (2) Center of Ophthalmology, IBILI, Faculty of Medicine, Coimbra, Portugal

Background and Aims: Patients with type 2 diabetes have an increased risk to develop cardiac ischemia and their response to such accidents is impaired. In the worst case, cardiac ischemia can lead to myocardial infarction,

causing death to nearly 75% of diabetic population. The high concentration of glucose in diabetic cells results in increasing concentration of a secondary metabolite, the methylglyoxal (MG) that is known to have deleterious effects. We believe that prolonged exposure to MG can induce, in normal subjects, changes similar to those that occur in diabetes. Therefore, we aimed to understand the role of MG on cardiac ischemia in diabetic and normal animal model.

Materials and Methods: We performed a comparative study between three groups: normal rats (W), type 2 diabetic non-obese Goto-Kakizaki rats (GK) and normal rats submitted to chronic administration of MG (WMG). Animals were sacrificed with 6 months of age, and their hearts were perfused in a Langerdorff system. At this point, hearts were submitted to different experimental conditions: control (c); ischemia (i) and ischemia-reperfusion (ir). Glycemic profile and several parameters in cardiac tissue were evaluated using mostly western blot technique.

Results: MG administration did not change glycemic profile in control animals. Comparing to W, plasmatic MG levels were higher in GK ($p<0.05$) and WMG ($p<0.05$); the cardiac MG levels were significantly higher in WMG ($p<0.001$). Looking to cardiac tissue staining of AGEs (Advanced Glycation End Products) and their receptors (RAGEs), it was observed an increasing fluorescence in GK and WMG groups. JNK protein expression particularly demonstrated a decreasing in (i)-subgroups among the three groups (W> GK>WMG); levels in WMG(ir) rats were also decreased ($p<0.001$) in comparison to W(ir). Phospho-JNK expression increased only in W(i) and GK(i) ($p<0.001$; $p<0.05$), comparing to their controls. All (ir)-subgroups showed P-JNK expression lower than their respective (c)-subgroups ($p<0.05$). Regarding to Akt protein, it levels decreased generally in (i)- and (ir)-subgroups among three groups. Levels of GK and WMG (c)-subgroups decreased in relation to W ($p<0.001$); the (i)-subgroups levels also decreased among the three groups ($p<0.01$; $p<0.05$), and (ir)-subgroup levels were only significantly lower in WMG ($p<0.05$). In phosphorilated form of Akt, it was observed decreasing levels in GK and WMG, when compared to W group: control ($p<0.001$; $p<0.01$); ischemic ($p<0.01$) and ischemic-reperfusion ($p<0.05$; $p<0.01$) subgroups. The ratio Bcl-2/Bax showed noteworthy an increase in W(i) and GK(i) comparing to their controls ($p<0.01$; $p<0.05$). WMG(i) showed a less increased ratio that was significantly lower than W(i) and GK(i) with $p<0.01$. Relating to W(c), GK and WMC (c)-subgroups decreased their values ($p<0.05$). Levels of Caspase 3 increased significantly in W(ir) and GK(ir) ($p<0.05$), comparing respectively with W(c) and GK(c). GK(ir) and WMG(ir) levels were higher than W(ir) ($p<0.05$).

Conclusion: The administration of methylglyoxal in normal rats is able to mimic the profile founded in diabetic rats and even some parameters are more impaired. Our results re-affirm the toxicity of the compound and demonstrate the potentiality of methylglyoxal to be a therapeutic target in diabetic cardiac ischemia disease

1260

Vascular actions of methylglyoxal with implications for endothelial dysfunction

C. M. Sena (1), P. Matafome (1), J. Crisóstomo (1), L. Rodrigues (1),
C. Bento (2), P. Pereira (2), R.M. Seiça (1)
(1) Institute of Physiology, IBILI, Faculty of Medicine, University of Coimbra, Coimbra, Portugal; (2) Center of Ophthalmology, IBILI, Faculty of Medicine, University of Coimbra, Coimbra, Portugal

Background and Aims: Modern diets can cause modern diseases. Research has linked a metabolite of sugar, methylglyoxal (MG), to the development of diabetic complications, but the exact mechanism has not been fully elucidated. The present study was designed to investigate whether MG could directly influence endothelial function, oxidative stress and inflammation in Wistar and Goto-kakizaki (GK) rats, an animal model of type 2 diabetes.

Materials and Methods: Wistar and GK rats treated with MG in the drinking water for 3 months were compared with the respectively control rats. The effects of MG were investigated on NO-dependent vasorelaxation in isolated rat aortic arteries from the different groups. Insulin resistance, NO bioavailability, glycation, a pro-inflammatory biomarker monocyte chemoattractant protein-1 (MCP-1) and vascular oxidative stress were also evaluated.

Results: Methylglyoxal treated Wistar rats significantly reduced the efficacy of NO-dependent vasorelaxation ($p<0.001$). This impairment was accompanied by a threefold increase in the oxidative stress marker nitrotyrosine. Advanced glycation endproducts (AGEs) formation was significantly increased as well as MCP-1 and the expression of the receptor for AGEs (RAGE). NO bioavailability was significantly attenuated and accompanied by an increase in superoxide anion immunofluorescence. Methylglyoxal treated GK rats significantly aggravated endothelial dysfunction, oxidative stress, AGEs accumulation and diminished NO bioavailability when compared with control GK rats.

Conclusion: These results indicate that methylglyoxal induced endothelial dysfunction in normal Wistar rats and aggravated the endothelial dysfunction present in GK rats. The mechanism is at least in part by increasing oxidative stress and/or AGEs formation with a concomitant increment of inflammation and a decrement in NO bioavailability. The present study provides further evidence for methylglyoxal as one of the causative factors in the pathogenesis of atherosclerosis and development of macrovascular diabetic complication.

1285

Neuronal and glial changes induced by type 1 diabetes in the rat hippocampus

J. M. Gaspar (1,2), F. I. Baptista (2), Á. F. Castilho (2), J. Liberal (2),
J. Gonçalves (3,4), A. F. Ambrósio (2,5)
(1) CEDOC, Faculdade Ciências Médicas, Lisbon, Portugal; (2) Centre of Ophthalmology and Vision Sciences, Coimbra, Portugal; (3) Laboratory of Pharmacology and Experimental Therapeutics, Coimbra, Portugal; (4) Institute of Biomedical Research on Light and Image (IBILI), Coimbra, Portugal; (5) Centre for Neuroscience and Cell Biology, Coimbra, Portugal

Background and Aims: Long-term diabetes can result in a variety of subtle cerebral disorders with manifestations demonstrated at structural, neurochemical, electrophysiological and neurobehavioural level. Cognitive and memory impairments associated with diabetes result from modification of hippocampal structure and function, including changes in neuronal and glial cells. The aim of this work was to further evaluate and identify changes in hippocampal neuronal and glial cells induced by diabetes at different time points along the early stages of the disease (two, four and eight weeks).

Materials and Methods: Diabetes was induced in male Wistar rats with a single intraperitoneal injection of streptozotocin. Neurodegeneration and apoptosis was evaluated by cresyl violet staining and detection of caspase-3. Neuronal changes were assessed by evaluating the immunoreactivity of microtubule associated protein-2 (MAP-2) and synaptophysin, as well as the protein content of Tuj-1, calbindin D28k and tau. Astrocyte reactivity was analyzed by measuring the content and immunoreactivity of glial fibrillary acidic protein (GFAP). Changes in microglial cells were evaluated with CD11b and ED1 markers.

Results: No signs of neurodegeneration or caspase-3 activation were detected in the hippocampus of diabetic animals. However, a decrease in the protein levels of all neuronal markers occurred after eight weeks of diabetes. Regarding MAP-2 immunoreactivity, there was a decrease in dentate gyrus at all time points of the study, and after eight weeks a decrease occurred in all hippocampal subregions (CA1, CA3 and dentate gyrus). Synaptophysin immunoreactivity increased in CA3 subregion at all time points. No changes were detected in astrocyte reactivity in diabetic animals. However, the number of activated microglia increased in dentate gyrus and CA3 subregion at eight weeks of diabetes.

Discussion: These observations indicate that diabetes does not induce neuronal degeneration in the hippocampus, at least during the early stages of the disease. However, neuronal changes occur, mainly after longer periods of diabetes (eight weeks), and CA3 subregion appears to be the most affected region. Moreover, astrocytes did not become reactive with diabetes, at least for the time points studied, but microglial cells became activated, suggesting the existence of a pro-inflammatory response. Altogether, these changes might affect cognitive and memory performance.